Luminescence of tetraphenylporphyrin by an energy transfer from photoexcited ZnO nanoparticle

Ichiro Hiromitsu[a,*], Ayana Kawami[a], Senku Tanaka[a], Shigekazu Morito[a], Ryo Sasai[a], Takahisa Ikeue[a], Yasuhisa Fujita[b], Makoto Handa[a]

[a] *Department of Material Science, Faculty of Science and Engineering, Shimane University, Matsue 690-8504, Japan*
[b] *Department of Electronic and Control Systems Engineering, Faculty of Science and Engineering, Shimane University, Matsue 690-8504, Japan*

Abstract

Photoluminescence (PL) properties of *meso*-tetraphenylporphine-4,4',4",4"'-tetracarboxylic acid ($H_2TPP(COOH)_4$) bound to ZnO nanoparticle were studied. With 1.2 $H_2TPP(COOH)_4$ molecules per ZnO particle, the PL intensity of $H_2TPP(COOH)_4$ with a 325 nm excitation was increased to a 3.2-times larger value by the conjugate formation with ZnO. The excitation spectrum of PL gave an evidence of an emission of $H_2TPP(COOH)_4$ by an energy transfer from ZnO. An analysis based on the Förster theory gave a reasonable value of 1.8 nm for the average distance between $H_2TPP(COOH)_4$ and emissive surface defects on the ZnO particle.

1. Introduction

The photophysical and photochemical properties of the conjugated systems of inorganic nanoparticles and organic molecules are gaining increasing interest for biomedical applications, e.g. imaging [1, 2, 3, 4, 5], and photodynamic therapy [6, 7, 8]. A key phenomenon for such applications is an energy transfer from inorganic nanoparticles to organic molecules and a resulting luminescence

*Corresponding author. Fax: +81 852 32 6409.
E-mail address: hiromitu@riko.shimane-u.ac.jp (I. Hiromitsu)

of the latter. Much effort is being made to obtain such a luminescence [9, 10, 11, 12, 13].

In our previous study [14], optical absorption and photoluminescence properties of a ZnO nanoparticle-porphyrin system were studied. ZnO is a direct band gap semiconductor with a band gap of 3.4 eV. Nanostructures of ZnO typically have a near-band-edge emission in the UV region and a defect-related visible emission in the blue to green region [15, 16, 17, 18]. Because of its potential of non-toxicity, ZnO is expected to be suitable for biomedical applications. Porphyrin, on the other hand, is a well-known emitter of red light. We tried to bind three types of porphyrins, 5-(4-aminophenyl)-10,15,20-triphenylporphyrin ($H_2TPP(NH_2)$), 5,10-bis(4-aminophenyl)-15,20-diphenylporphyrin ($H_2TPP(NH_2)_2$), and {5,10-bis(4-aminophenyl)-15,20-diphenylporphyrinato}zinc(II) ($ZnTPP(NH_2)_2$), to the ZnO particles dispersed in diethylene glycol, using L-cysteine ($HS\text{-}CH_2CH(NH_2)\text{-}COOH$) as a linker. It was expected that ZnO-(L-cysteine)-porphyrin linkage might be formed by a Zn-S bonding between ZnO and L-cysteine and a -(CO)-(NH)-bonding between L-cysteine and porphyrin [8]. It was shown, however, that the ZnO-(L-cysteine) bonding was not formed, so that ZnO and porphyrin were not bound to each other in the previous systems [14]. Nevertheless, an energy transfer from photoexcited ZnO to porphyrins occurred which probably was a collision-controlled process. However, the transferred energy was not spent for the emission of porphyrins.

In the present study, we used *meso*-tetraphenylporphine-4,4',4",4"'-tetracarboxylic acid ($H_2TPP(COOH)_4$) shown in Fig. 1(a), and linked $H_2TPP(COOH)_4$ to ZnO nanoparticle by a dehydration between the carboxyl groups of porphyrin and the hydroxyl groups on the surface of ZnO. Generally, there are three possible binding modes between carboxyl group and metal atoms [16, 19, 20, 21], i.e. unidentate, chelating and bridging, as shown in Fig. 1(b). Although determination of the binding mode is usually difficult, the usage of carboxyl group to link organic molecules to the surface of inorganic semiconductor is a quite popular technique [22, 23, 24, 25]. Dye-sensitized solar cell is a typical example that uses this type of linkage to achieve photo-induced electron transfer from

dye molecule to metal oxide [20, 21]. On the other hand, usage of this type of linkage to achieve energy transfer between organic molecule and inorganic semiconductor has been rarely reported. To our knowledge, a paper by Ren et al.[26] is the only example of such usage. They reported an excitation energy transfer in CdSe/ZnS quantum dot-organic dye conjugates in which the linkage between the two was made by using the carboxyl groups in the dye molecule. The present study will provide another example. It will be shown that $H_2TPP(COOH)_4$ is linked to ZnO particle by its carboxyl groups and an excitation energy transfer occurs from ZnO to $H_2TPP(COOH)_4$ resulting in a luminescence of the latter.

2. Experimental

$Zn(OAc)_2{\cdot}2H_2O$ (Reagent grade, Kanto), $LiOH{\cdot}H_2O$ (Reagent grade, Wako) and ethanol (Spectrophotometric grade, Wako) were used without further purification. $H_2TPP(COOH)_4$ was purchased from Aldrich and used after recrystallization from reagent grade ethanol.

ZnO nanoparticles were synthesized by the method of Spanhel and Anderson [27, 28] with modification. 9.1×10^{-3} mol of $Zn(OAc)_2{\cdot}2H_2O$ was dissolved in 200 ml of reagent grade methanol. Although ethanol is usually used as the solvent for ZnO synthesis, we used methanol because the precipitation of the synthesized ZnO particles by centrifugation became easier. To the methanol solution of $Zn(OAc)_2$, 2.7×10^{-2} mol of $LiOH{\cdot}H_2O$ was slowly added under stirring. When all the $LiOH{\cdot}H_2O$ was added, white suspension was obtained indicating a generation of ZnO. The obtained ZnO was washed by the following procedure. After adding 150 ml of reagent grade heptane, the suspension was centrifuged at 3000 rpm. The precipitate was dispersed in 150 ml of methanol, and refluxed at 55°C for 24 hr under stirring. The process of the centrifugation and refluxing was repeated once again. The suspension was again centrifuged at 3000 rpm, and the precipitate was dispersed in 150 ml of methanol. Then, the dispersion was separated into 100 ml and 50 ml. The latter was centrifuged at 13000 rpm, and the precipitate was dried on a hot plate of 80°C within 30 min. The weight of the dried ZnO powder was 0.10 g, indicating that the yield of the

ZnO synthesis was 41%. It is noted that the drying process should not exceed 30 min, otherwise the particle size of ZnO increases. From the weight of the dried ZnO powder, the concentration of ZnO in the dispersion was calculated to be 2.5×10^{-2} mol/L.

The synthesis of ZnO-H_2TPP(COOH)$_4$ conjugates was carried out as follows. First, the ZnO dispersion in methanol was centrifuged at 13000 rpm, and the methanol was exchanged by ethanol of spectrophotometric grade, and the concentration of ZnO was adjusted to 5.0×10^{-4} mol/L (A). On the other hand, H_2TPP(COOH)$_4$ was dissolved into ethanol of spectrophotometric grade with a concentration of 4.5×10^{-6}, 9.0×10^{-6} or 1.8×10^{-5} mol/L (B). To 1 ml of B, 6 ml of A was added. Then, the mixture was sonicated for 30 sec, and kept at room temperature overnight to complete the ZnO-porphyrin linkage. After keeping the dispersion a few days, the conjugates were precipitated with the supernatant having no color, which indicates that no H_2TPP(COOH)$_4$ exists in the supernatant. This is an evidence that H_2TPP(COOH)$_4$ molecules are bound to the ZnO particles. The final concentration of H_2TPP(COOH)$_4$ in the dispersion was 6.4×10^{-7}, 1.3×10^{-6} or 2.6×10^{-6} mol/L, and that of ZnO was 4.3×10^{-4} mol/L. Since the present ZnO particles have a spherical shape with a diameter of 3.3 nm, as shown in the next section, the average number of H_2TPP(COOH)$_4$ molecules per ZnO particle was calculated to be 1.2, 2.4 or 4.8, using the density 5.78 of ZnO. For the infrared absorption measurement, conjugates with 5.0 porphyrin molecules per ZnO particle were prepared, which were then centrifuged and dried on a hot plate of 80°C within 30 min.

X-ray diffraction (XRD) of the ZnO particles was measured using Rigaku RINT2100 diffractometer with Ni-filtered Cu-$K\alpha$ radiation. Transmission electron microscopic (TEM) observation of the ZnO particles was performed on JEOL JEM-2010. Infrared (IR) absorption spectra were measured on JASCO FT-IR 660 plus spectrometer with samples homogeneously dispersed in KBr pellets. Ultraviolet-visible (UV-vis) absorption spectra were measured on Shimadzu UV-3100PC. Photoluminescence (PL) spectra were measured on OCEAN OPTICS USB2000 with an excitation light of $\lambda = 325$ nm from a He-Cd laser

whose intensity was attenuated to 22 μW to prevent saturation of the PL intensity. Excitation spectra of PL were measured on HORIBA FluoroMax-4. The UV-vis absorption and emission measurements were performed using a 10 mm $\times$ 2 mm quartz cell. For the UV-vis absorption, the path length of the penetrating light through the sample was 2 mm. For the emission measurements, the path length of the excitation light was 10 mm, and the emitted light was detected at right angles to the excitation beam. A long pass filter with a cut-on wavelength of 390 nm was used for the detection of emitted light to remove the excitation light. The emission quantum yield of ZnO particles was measured on HAMAMATSU C9920-02 using a 10 mm $\times$ 10 mm quartz cell.

3. Results and discussion

3.1. XRD and TEM observation of ZnO particles

Fig. 2 shows the XRD pattern of the ZnO nanoparticles, which is identical with a reported one for ZnO with Wurtzite structure [29, 30]. From the line width of the (102) reflection at 47.7°, the particle size was estimated to be 3.3 $\pm$ 0.5 nm using the Scherrer's formula [31],

$$t = \frac{0.9\,\lambda}{B\cos\theta_B}, \tag{1}$$

where t is the diameter of the particle, λ is the wavelength of the X ray, B is the line broadening at half maximum of the diffraction peak in radian, and θ_B is the Bragg angle of the diffraction peak.

Fig. 3 shows the TEM image of the ZnO nanoparticles. It is observed that the ZnO particles are nearly spherical and tend to be agglomerated. The observed particle size is in agreement with that estimated by XRD.

3.2. IR absorption spectra

IR absorption spectra were measured to study the features of the $H_2TPP(COOH)_4$-ZnO binding. Fig. 4 shows the IR spectra of tetraphenylporphyrin(H_2TPP), $H_2TPP(COOH)_4$, ZnO particles, and ZnO-$H_2TPP(COOH)_4$ conjugates. In the IR spectrum of $H_2TPP(COOH)_4$ (Fig. 4(b)), the peaks for the C=O and C−O

stretchings of carboxyl groups are observed at 1700 and 1260 cm^{-1}, respectively [20, 21], which are absent in the IR spectrum of H_2TPP (Fig. 4(a)) as expected. In the IR spectrum of ZnO-$H_2TPP(COOH)_4$ conjugates (Fig. 4(d)), no peaks at either 1700 or 1260 cm^{-1} are observed. This is an indication of the ZnO-$H_2TPP(COOH)_4$ binding through the carboxyl groups for the following reason. When a carboxyl group is bound to ZnO by any of the three binding modes in Fig. 1(b), the IR peaks of the C=O and C−O stretchings should disappear and, instead, two peaks for the asymmetric and symmetric stretchings of CO_2 should appear in the region 1650-1400 cm^{-1}. Reported $\nu_{asym}(CO_2)$ and $\nu_{sym}(CO_2)$ are 1577 and 1425 cm^{-1}, respectively, in the unidentate mode, 1550 and 1456 (or 1405) cm^{-1} in the chelating mode, and 1600 and 1441 cm^{-1} (or 1639 and 1489 cm^{-1}) in the bridging mode [19]. Unfortunately, the peaks for $\nu_{asym}(CO_2)$ and $\nu_{sym}(CO_2)$ are not identified in Fig. 4(d) because of an overlapping of the peaks coming from ZnO particles and porphyrin rings. Nevertheless, the disappearance of the C=O and C−O stretching peaks at 1700 and 1260 cm^{-1} strongly suggests that all the carboxyl groups in $H_2TPP(COOH)_4$ were used for the linkage with ZnO particles.

3.3. UV-vis absorption and emission spectra

3.3.1. ZnO nanoparticles

Fig. 5 shows the UV-vis absorption, PL, and excitation spectra of the ZnO nanoparticles in ethanol. The onset of the UV-vis absorption locates at 350 nm, which was red-shifted to 380 nm when the particle size was increased to 10.8 nm. The PL spectrum of ZnO particles has a broad peak at 537 nm, which is attributed to an emission from surface defects [15, 16, 17, 18]. The excitation spectrum resembles the absorption spectrum as expected.

3.3.2. ZnO-H_2TPP(COOH)$_4$ conjugates

Fig. 6(a) shows the UV-vis absorption spectrum of ZnO-$H_2TPP(COOH)_4$ conjugates in ethanol with 1.2 porphyrin molecules per ZnO particle (Conjugate A), as well as the absorption spectra of $H_2TPP(COOH)_4$ and ZnO particles in ethanol. The absorption spectrum of the conjugates is a sum of the absorption

spectra of ZnO and porphyrin as expected. However, the absorption peaks of porphyrin are slightly red-shifted and the peak intensities become lower by the conjugate formation: The B band [32, 33] at 417 nm is red-shifted by 3 nm, and the Q bands [32, 33] at 500-670 nm are shifted by $2 \sim 4$ nm. A much larger red shift has been reported for ZnO nanotetrapod-protoporphyrin conjugates in which the B band was shifted by as much as 84 nm [23]. This was attributed to a π-π stacking interaction between the porphyrin rings. The red shift of 3 nm in the present system, however, is not attributed to the inter-ring interaction because the degree of the red shift did not depend on the concentration of porphyrins: The conjugates with 2.4 or 4.8 porphyrin molecules per ZnO particle also showed a red shift of 3 nm. The most probable origin of the red shift is an interaction between the porphyrin ring and the ZnO particle, the detailed mechanism of which is unknown at present.

Fig. 6(b) shows the PL spectrum of Conjugate A in ethanol, as well as the PL spectra of $H_2TPP(COOH)_4$ and ZnO particles in ethanol with the same concentrations with Conjugate A, i.e., 6.4×10^{-7} and 4.3×10^{-4} mol/L for $H_2TPP(COOH)_4$ and ZnO, respectively. It is observed in Fig. 6(b) that the PL intensity of ZnO at 537 nm is decreased to 27% of its original value and that of $H_2TPP(COOH)_4$ at 650 nm is increased to a 3.2-times larger value by the conjugate formation. This suggests that an energy transfer from ZnO to porphyrin occurred and the transferred energy was spent for the emission of the latter.

Fig. 7 shows the excitation spectra of Conjugate A with the detection wavelengths ($\lambda_{\rm detect}$) of 649 and 540 nm. As shown in Fig. 6(b), the emission of Conjugate A at 540 nm consists solely of the ZnO emission, while the emission at 649 nm consists mainly of the porphyrin emission with a minor contribution from the ZnO emission. As observed in Fig. 7, the excitation spectrum for $\lambda_{\rm detect} = 649$ nm has a large peak at 417 nm corresponding to the B-band absorption of porphyrin and a peak at 320 nm corresponding to the exciton absorption of ZnO. A crucial question is whether the exciton peak at 320 nm for $\lambda_{\rm detect} = 649$ nm comes from the porphyrin emission or ZnO emission. A

comparison with the excitation spectrum with $\lambda_{\mathrm{detect}} = 540$ nm provides an answer to this question. The peak intensity at 320 nm for $\lambda_{\mathrm{detect}} = 649$ nm is much larger than that for $\lambda_{\mathrm{detect}} = 540$ nm. On the other hand, since the emission intensity of ZnO at 649 nm is weaker than that at 540 nm as shown in Fig. 6(b), the excitation spectrum with $\lambda_{\mathrm{detect}} = 649$ nm should have a smaller contribution of the ZnO emission than that with $\lambda_{\mathrm{detect}} = 540$ nm. Thus, it is concluded that the exciton peak of ZnO at 320 nm for $\lambda_{\mathrm{detect}} = 649$ nm in Fig. 7 mainly comes from the porphyrin emission. This is a clear evidence of an energy transfer from ZnO to porphyrin and a resulting emission of the latter.

For the ZnO-H_2TPP(COOH)$_4$ conjugates with 2.4 and 4.8 porphyrin molecules per ZnO particle (Conjugate B and C), a similar exciton peak of ZnO was observed in the excitation spectrum with $\lambda_{\mathrm{detect}} = 649$ nm. This indicates that the emission of porphyrin by the energy transfer from ZnO still occurs in Conjugate B and C. For Conjugate B, the emission intensity of porphyrin was increased to a 2.5-times larger value by the conjugate formation. However, for Conjugate C, it was decreased by the conjugate formation. The decrease in the emission intensity may be attributed to a deactivation of some of the porphyrin molecules by an interaction with their environment [34], the detailed mechanism of which is unknown at present.

3.4. On the mechanism of energy transfer

The energy transfer between inorganic semiconductor and organic molecule is usually explained by the Förster mechanism [35], in which the rate of energy transfer from an energy donor to an acceptor, $k_T(r)$, is given by the following formula.

$$k_T(r) = \frac{1}{\tau_D}\left(\frac{R_0}{r}\right)^6, \tag{2}$$

where τ_D is the decay time of the donor in the absence of acceptor, R_0 is the Förster distance, and r is the donor-acceptor distance. Hence, when $r = R_0$, the rate of transfer is equal to $1/\tau_D$. R_0 is given by the following formula.

$$R_0 = \left(\frac{9000\,(\ln 10)\,\kappa^2\,Q_D}{128\,\pi^5\,N_A\,n^4}\,J\right)^{1/6}, \tag{3}$$

where κ is a parameter describing the relative orientation between the transition dipoles of the donor and acceptor, Q_D is the quantum yield of the donor emission in the absence of acceptor, N_A is Avogadro's number, n is the refractive index of the medium, and J is the overlap integral defined by

$$J = \int_0^\infty F_D(\lambda)\, \epsilon_A(\lambda) \lambda^4 d\lambda \,. \tag{4}$$

In Eq. (4), $F_D(\lambda)$ represents the emission intensity of the donor in the wavelength range between λ and $\lambda + \Delta\lambda$ with the total intensity normalized to unity, and $\epsilon_A(\lambda)$ is the extinction coefficient of acceptor at λ. Using the PL spectrum of ZnO in Fig. 5 and the absorption spectrum of porphyrin in Fig. 6(a), J was calculated to be 5.3×10^{14} $\mathrm{M^{-1}cm^{-1}nm^4}$ [35], which is mainly determined by an overlap between the Q bands of porphyrin and the emission spectrum of ZnO. Using a measured value of $Q_D = 0.01$, and assuming $\kappa^2 = 2/3$ for random orientation of the transition dipoles and $n = 1.4$ [35], R_0 is calculated to be 2.1 nm.

The energy transfer efficiency E is calculated from the experimental results by the following formula [26, 35].

$$E = 1 - \frac{F}{F_0} \,, \tag{5}$$

where F and F_0 are the emission intensities of the donor (ZnO) with and without the acceptor (porphyrin), respectively. On the other hand, E is theoretically expressed by the following formula [1, 36].

$$E = \frac{N k_T}{N k_T + (1/\tau_D)} = \frac{N}{N + (r/R_0)^6} \,, \tag{6}$$

where N is the number of porphyrin molecules per ZnO particle. Using Eqs. (5) and (6), the following Stern-Volmer relationship is obtained [26, 35].

$$\frac{F_0}{F} - 1 = \frac{N}{(r/R_0)^6} \,. \tag{7}$$

Fig. 8 shows the Stern-Volmer plot obtained from the present experimental results. As expected by Eq. (7), the experimental Stern-Volmer plot has a linear dependence on N. From the slope $1/(r/R_0)^6 = 2.6$ of the plot, r is estimated

to be 1.8 nm, which should be the average distance between porphyrin and the emissive surface defects of ZnO particle. Since the distance between the center of the porphyrin ring and the surface of the ZnO particle should be roughly 1 nm and the particle size of ZnO is 3.3 nm, the estimated value of $r = 1.8$ nm may be reasonable. This result supports that the energy transfer in the present system is caused by the Förster mechanism.

The present energy transfer occurs due to the overlapping between the emission spectrum of ZnO and the very weak Q-band absorption of porphyrin at 500∼670 nm, but the very strong B-band absorption at 417 nm is not used for the transfer. The overlap between the B band and the emission spectrum of ZnO should be increased to get a more efficient energy transfer, which is a subject of future study.

In the present system, no *electron* transfer occurs between ZnO and porphyrin, which can be explained by the energy levels of the conduction-band edge of ZnO and the lowest-unoccupied molecular orbital (LUMO) of porphyrin molecule. The conduction-band edge of ZnO locates at 4.4 eV. On the other hand, LUMO level of porphyrin locates at 4.5 eV, estimated from the highest-occupied molecular orbital (HOMO) level of 6.4 eV for H_2TPP in gas phase [37] and optical HOMO-LUMO gap of 1.9 eV. Since the conduction band edge of ZnO and the LUMO level of porphyrin locate very close to each other, no efficient electron transfer occurs in the present system.

4. Conclusions

ZnO-H_2TPP$(COOH)_4$ conjugates were successfully synthesized. The porphyrin is linked to the ZnO particle through the carboxyl groups of the former. It was found that an excitation energy transfer from ZnO to porphyrin causes an emission of the latter. By the Förster theory, the average distance between H_2TPP$(COOH)_4$ and emissive surface defects of the ZnO particle was estimated to be 1.8 nm, which is a reasonable value because the H_2TPP$(COOH)_4$ molecule and the ZnO particle are directly linked to each other. This supports that the energy transfer in the present system is caused by the Förster mechanism.

Acknowledgment

The TEM observation of ZnO particles were performed at Center for Integrated Research in Science, Shimane University.

References

[1] A.R. Clapp, I.L. Medintz, J.M. Mauro, B.R. Fisher, M.G. Bawendi, H. Mattoussi, J. Am. Chem. Soc. 126 (2004) 301.

[2] A. Dorfman, N. Kumar, J. Hahm, Adv. Mater. 18 (2006) 2685.

[3] X. Cao, C.M. Li, H. Bao, Q. Bao, H. Dong, Chem. Mater. 19 (2007) 3773.

[4] A. Dif, E. Henry, F. Artzner, M. Baudi-Floc'h, M. Schmutz, M. Dahan, V. Marchi-Artzner, J. Am. Chem. Soc. 130 (2008) 8289.

[5] J. Chen. F. Zeng, S. Wu, Q. Chen, Z. Tong, Chem. Eur. J. 14 (2008) 4851.

[6] A.C.S. Samia, X. Chen, C. Burda, J. Am. Chem. Soc. 125 (2003) 15736.

[7] I. Roy, T.Y. Ohulchanskyy, H.E. Pudavar, E.J. Bergey, A.R. Oseroff, J. Morgan, T.J. Dougherty, P.N. Prasad, J. Am. Chem. Soc. 125 (2003) 7860.

[8] Y. Liu, Y. Zhang, S. Wang, C. Pope, W. Chen, Appl. Phys. Lett. 92 (2008) 143901.

[9] S. Dayal, Y. Lou, A.C.S. Samia, J.C. Berlin, M.E. Kenney, C. Burda, J. Am. Chem. Soc. 128 (2006) 13974.

[10] M. Idowu, J.-Y. Chen, T. Nyokong, New J. Chem. 32 (2008) 290.

[11] A.A.R. Neves, A. Camposeo, R. Cingolani, D. Pisignano, Adv. Funct. Mater. 18 (2008) 751.

[12] S. Moeno, T. Nyokong, Polyhedron 27 (2008) 1953.

[13] A.M.-C. Ng, A.B. Djurišić, K.-H. Tam, W.-M. Kwok, W.-K. Chan, W.Y. Tam, D.L. Phillips, K.-W. Cheah, Adv. Funct. Mater. 18 (2008) 566.

[14] I. Hiromitsu, T. Ikeue, K. Karino, T. Ohno, S. Tanaka, H. Shiratori, S. Morito, Y. Fujita, M. Handa, Chem. Phys. Lett. 474 (2009) 315.

[15] K. Vanheusden, W.L. Warren, C.H. Seager, D.R. Tallant, J.A. Voigt, B.E. Gnade, J. Appl. Phys. 79 (1996) 7983.

[16] S. Sakohara, M. Ishida, M.A. Anderson, J. Phys. Chem. B 102 (1998) 10169.

[17] F.H. Letter, H.R. Alves, A.Hofstaetter, D.M. Hofmann, B.K. Meyer, Phys. Stat. Sol. B 226 (2001) R4.

[18] N.S. Norberg, D. R. Gamelin, J. Phys. Chem. B 109 (2005) 20810.

[19] G.B. Deacon, R.J. Phillips, Coord. Chem. Rev. 33 (1980) 227.

[20] K.S. Finnie, J.R. Bartlett, J.L. Woolfrey, Langmuir 14 (1998) 2744.

[21] O. Taratula, E. Galoppini, D. Wang, D. Chu, Z. Zhang, H. Chen, G. Saraf, Y. Lu, J. Phys. Chem. B 110 (2006) 6506.

[22] Y.L. Wu, A.I.Y. Tok, F.Y.C.Boey, X.T. Zeng, X.H. Zhang, Appl. Surf. Sci. 253 (2007) 5473.

[23] D. Liu, W. Wu, Y. Qiu, S. Yang, S. Xiao, Q. Wang, L. Ding, J. Wang, Langmuir 24 (2008) 5052.

[24] K. Senthilkumar, O. Senthilkumar, K. Yamauchi, M. Sato, S. Morito, T. Ohba, M. Nakamura, Y. Fujita, Phys. Stat. Sol. B 246 (2009) 885.

[25] M. Sato, H. Harada, S. Morito, Y. Fujita, S. Shimosaki, T. Urano, M. Nakamura, Appl. Surf. Sci. 256 (2010) 4497.

[26] T. Ren, P.K. Mandal, W. Erker, Z. Liu, Y. Avlasevich, L. Puhl, K. Müllen, T. Basché, J. Am. Chem. Soc. 130 (2008) 17242.

[27] L. Spanhel, M.A. Anderson, J. Am. Chem. Soc. 113 (1991) 2826.

[28] E.A. Meulenkamp, J. Phys. Chem. B 102 (1998) 5566.

[29] T. Andelman, Y. Gong, M. Polking, M. Yin, I. Kuskovsky, G. Neumark, S. O'Brien, J. Phys. Chem. B 109 (2005) 14314.

[30] X. Zhong, W. Knoll, Chem. Commun. (2005) 1158.

[31] B.D. Cullity, Elements of X-ray diffraction, 2nd ed. Addison-Wesley, Reading, Massachusetts, 1978, Chap. 9.

[32] M. Gouterman, The Porphyrins 3 (1978) 1.

[33] M. Gouterman, J. Mol. Spectrosc. 6 (1961) 138.

[34] L. Oddos-Marcel. F. Madeore, A. Bock, D. Neher, A. Ferencz, H. Rengel, G. Wegner, C. Kryschi, H.P. Trommsdorff, J. Phys. Chem. 100 (1996) 11850.

[35] J. R. Lakowicz, Principles of Fluorescence Spectroscopy, 3rd ed. Springer, New York, 2006, Chap. 13.

[36] A.R. Clapp, I.L. Medintz, H. Mattoussi, Chem. Phys. Chem. 7 (2006) 47.

[37] S.C. Khandelwal, J.L. Roebber, Chem. Phys. Lett. 34 (1975) 355.

Figure 1: (a) A proposed linkage between ZnO nanoparticle and $H_2TPP(COOH)_4$. (b) Three binding modes between carboxyl group and Zn atoms.

Figure 2: XRD pattern of ZnO nanoparticles.

Figure 3: TEM image of ZnO nanoparticles. The white circle shows a single particle.

Figure 4: IR absorption spectra of (a) H_2TPP, (b) $H_2TPP(COOH)_4$, (c) ZnO particles, and (d) ZnO-$H_2TPP(COOH)_4$ conjugates (5.0 porphyrin molecules per ZnO particle).

Figure 5: UV-vis absorption (with light path length = 2 mm), photoluminescence (with λ_{excite} = 325 nm), and excitation spectrum of photoluminescence (with λ_{detect} = 540 nm), of ZnO nanoparticles dispersed in ethanol (4.3×10^{-4} mol/L).

Figure 6: UV-vis absorption spectra (a) and photoluminescence spectra (b) of ZnO-$H_2TPP(COOH)_4$ conjugates (1.2 porphyrin molecules per ZnO particle) dispersed in ethanol, $H_2TPP(COOH)_4$ solution in ethanol, and ZnO nanoparticles dispersed in ethanol. The concentrations of ZnO and $H_2TPP(COOH)_4$ are 4.3×10^{-4} and 6.5×10^{-7} mol/L, respectively. The light path length for (a) was 2 mm. λ_{excite} for (b) was 325 nm.

Figure 7: Excitation spectra of photoluminescence of ZnO-$H_2TPP(COOH)_4$ conjugates (1.2 porphyrin molecules per ZnO particle) dispersed in ethanol. λ_{detect} = 649 and 540 nm.

Figure 8: Stern-Volmer plot for ZnO-$H_2TPP(COOH)_4$ conjugates. F and F_0 are the emission intensities of ZnO with and without $H_2TPP(COOH)_4$, respectively.

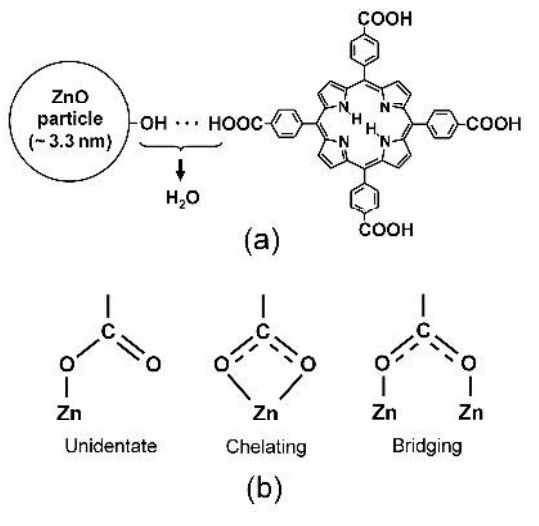

Fig. 1 "Conjugate"

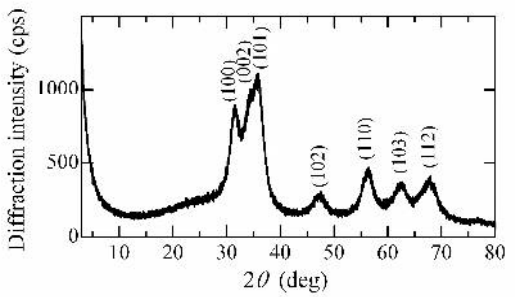

Fig. 2 "XRD"

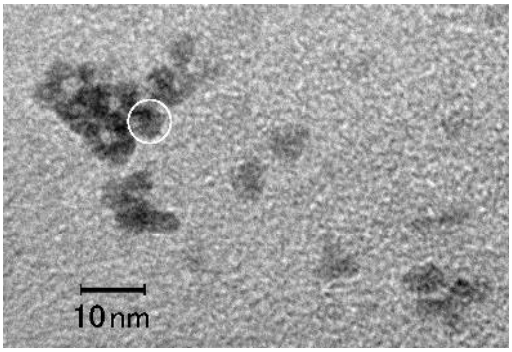

Fig. 3 "TEM"

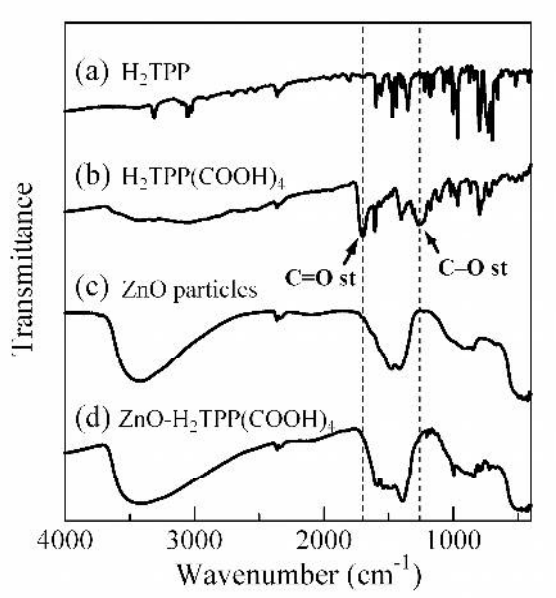

Fig. 4 "IR"

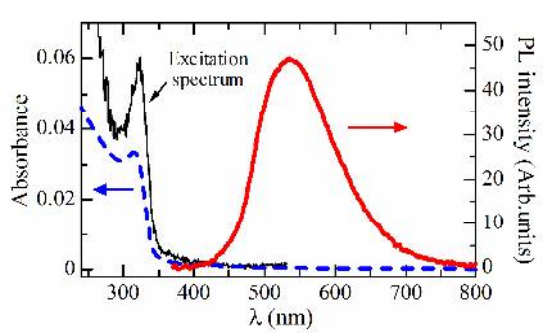

Fig. 5 "ZnO"

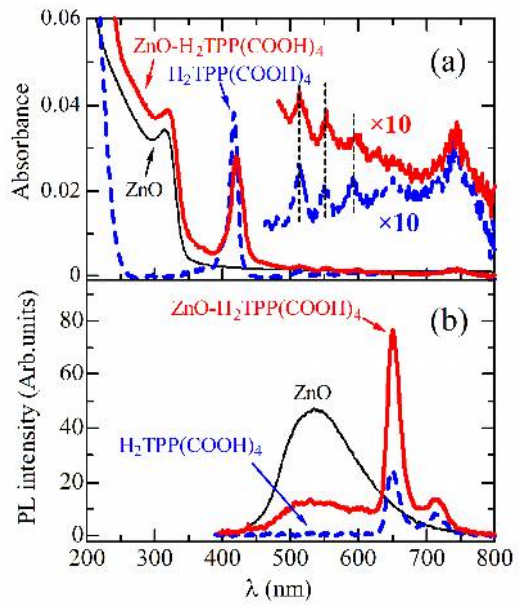

Fig. 6 "Abs_PL1"

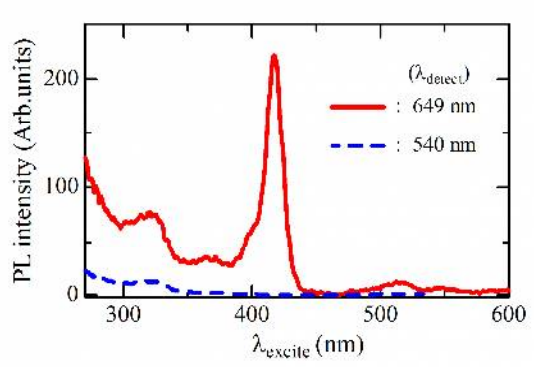

Fig. 7 "Exci1"

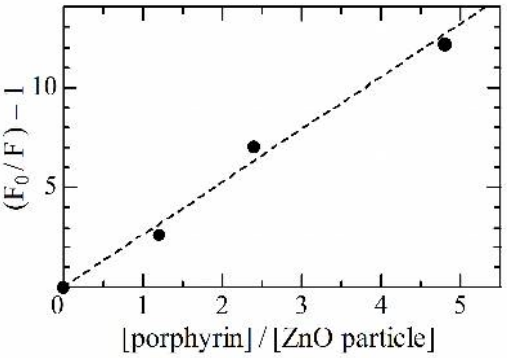

Fig. 8 "Stern"